Journal of Engineering and Applied Sciences 11 (3): 322-327, 2016
ISSN: 1816-949X

Application of X-Ray Microtomography in Calculating the Filtration Characteristics of Porous Media

[1, 2]Timur Rustamovich Zakirov, [1]Akhmet Askhatovich Galeev,
[1]Korolev Eduard Anatolievich, [1] Ildar Saiakhovich Nuriev and [1]Evgenii Olegovich Statsenko
[1]Kazan (Volga Region) Federal University, Kazan, Russia
[2]Federal State Budgetary Institution of Science "Institute of Mechanics and
Mechanical Engineering, Kazan Scientific Center, Russian Academy of Sciences", Kazan, Russia

Abstract: This study deals with the problem of application of X-ray microtomography in calculating the absolute permeability coefficient of cores of oil reservoirs. To simulate the process of fluid flow using the digital tomographic images of pore channels both the continuity equation and stationary Navier-Stokes equations were used. Researchers compared the filtration characteristics of porous media calculated on the basis of the model proposed in this study with the permeability coefficients calculated by the Kozeny-Carman equation. We have shown that the permeability coefficients calculated by the Kozeny-Carman equation give higher values as compared with the filtration characteristics calculated by both the Navier-Stokes equation and the continuity equation. We have revealed that the reservoir properties of cores, calculated on the basis of microtomographic data can be extrapolated to the samples of larger porous media.

Key words: X-ray micro-CT, absolute permeability coefficient, modeling, sandstone, fluid flow

INTRODUCTION

Describing the properties of core material plays an important role in assessing the resources of the test field, calculating hydrocarbon reserves and justifying the chosen way of development of oil and gas deposits (Nikolaevskii, 1996). Unlike the parameters such as porosity, pore surface area and permeability coefficient that can be directly measured and described by numerical values, the investigation of the geometry of pore channels is only possible with the use of modern technology.

Methods of X-ray tomography used for obtaining digital three-dimensional images of the internal structure of porous media of submicron and nanometer geometrical resolution have been successfully developed in recent years. Application of this method in studying the reservoir properties of porous media was discussed in detail in the studies (Blunt *et al*., 2013; Andrew *et al*., 2014; De Boever *et al*., 2012; Wennberg *et al*., 2009; Watanabe *et al*., 2011; Farber *et al*., 2003; Mathews *et al*., 2011; Kuper *et al*., 2007).

X-ray tomography is used in the simulation of pore-scaled filtration processes which allows us not only to obtain information on the channels open degree by analyzing the field of fluid velocity but also to measure the filtration characteristics of the test samples (Mostaghimi *et al*., 2013; Dvorkin *et al*., 2008). This approach to the calculation of permeability coefficient is more accurate than the Kozeny-Carman Model which is not universal for all types of porous media (Mostaghimi *et al*., 2013; Romm, 1985; Bulgakov *et al*., 2010). This fact makes the calculation of the filtration characteristics of the cores using the methods of X-ray tomography and mathematical modeling an important and urgent process.

Objects of research: The samples presented were core material of oil sandstones of the Permian and Carboniferous age from Melekesskian depression of Volga-Ural anteclise.

Sandstone is a polymineral, slightly calcareous, unequally oil-saturated in its composition with small-medium-grained structure with silty areas. According to the petrographic analysis, 85-90% of sandstones consist of fragments of minerals and rocks and 10-15% cementing agent.

Pore-scaled simulation of filtration process

X-ray computed microtomography: The cores were measured with the use of micro/nanofocal X-ray monitoring system for computed tomography and 2D inspection Phoenix v|tome|x s240. All measurements were carried out with the use of nanofocal X-ray tube. Pictures of core samples were taken at an accelerating voltage of

Corresponding Author: Timur Rustamovich Zakirov, Kazan (Volga Region) Federal University, Kazan, Russia

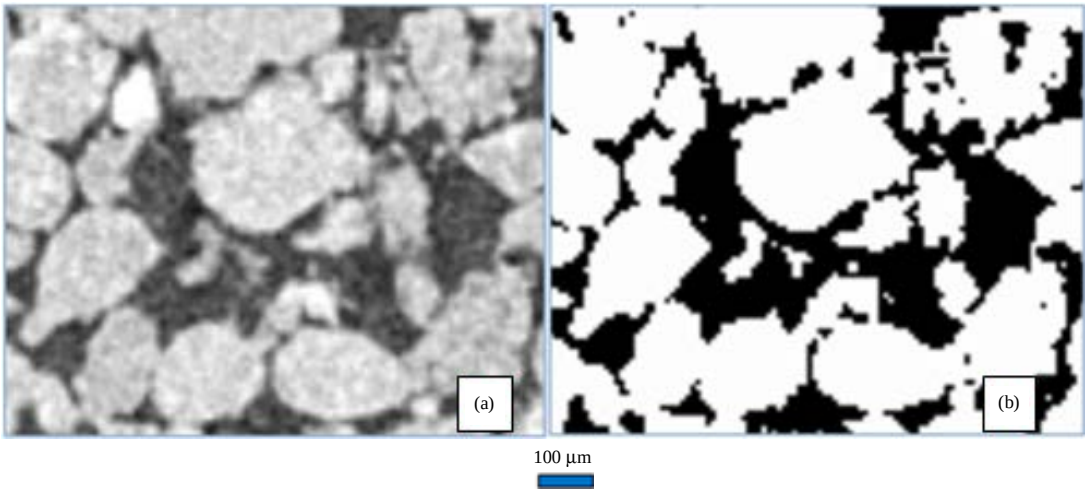

Fig. 1: Fragment of tomogram cross-section: a) original image and b) image after segmentation

120 kV and a current of 90 µA of the X-ray tube. A double shooting was conducted for each sample: using cylinders with diameter of 30 mm and length of 40 mm and parallelepipeds of 10×4×4 mm, cut out of these cylinders.

Preliminary computed processing, segmentation (Iassonov *et al*., 2009) and analysis of the geometric characteristics of the tomograms were carried out with Avizo Fire Edition (Visualization Sciences Group) program.

Figure 1a shows a fragment of the original tomogram, taken with a resolution of 10 µm where the black color items refer to areas with the lowest attenuation of X-rays, and the lighter shades of gray refer to areas with higher attenuation ability. Figure 1b shows the same fragment of the sample after the procedure of image segmentation into two phases: pores and a skeleton.

The results of the image processing are used in the analysis of porous structure of cores as well as to set boundary conditions in the solid areas upon modeling the filtration flows.

MATERIALS AND METHODS

Mathematical model of viscous fluid flow in pores: The process of fluid flow in the pore space is described as the Eq. 1 of continuity and the stationary Navier-Stokes Eq. 2 (Loitsianskii, 1973). The statement of the stationarity of fluid flow relies upon the results of study (Mostaghimi *et al*., 20113) which show that the flow rate at low differential pressures (several kPa) is very slow (tens of mm/c). Hence, the inertial forces in comparison with diffusion ones can be disregarded within the framework of the current problem:

$$\mathrm{div}U = 0 \tag{1}$$

$$\mu\Delta U = \frac{1}{\rho}\nabla P \tag{2}$$

Where:

P = The pressure field
U (u, v, w) = The velocity field
ρ = Fluid density
µ = Fluid viscosity

Both pressure and speed in the formulation of the problem are functions that depend on the cell coordinates of the core digital image

Using Eq. 1 and 2 to describe the motion of the fluid in porous media differs from the approach discussed in (Zakirov and Nikiforov, 2014; Nikiforov *et al*., 2015; Zakirov *et al*., 2015; Zakirov and Nikiforov, 2013, 2012) where the fluid flow is described by the equations of continuity where the coefficients of porosity and permeability are average values in terms of volume.

Sampling of the equation system is carried out by the finite difference method (Belotserkovskii, 1994; Gosmen *et al*., 1972) and gridding is done by the method of Markers And Cells (MAC) (Belotserkovskii, 1994; Roach,1980; Bear, 1972). The cell structure in the MAC method is constructed in such way that the pressure $P_{i,\ j,\ k}$ is determined in the center and the velocity components, e.g., $u_{i-1/2,\ j,\ k}$ and $u_{i+1/2,\ j,\ k}$ in the center of its left and right face, respectively. The result of solving a matrix equation obtained from the sampling can be found with the help of SPARSKIT library: the process uses ILU-decomposition (ILUT procedure) and the iterated method of solution (BCGSTAB and GMRES procedures) (Saad, 2003). No-slip and impermeability conditions are

applied to the external boundaries and solid surfaces inside the equilibration region (Saad, 2003). The following parameters values were taken for the fluid model: viscosity $\mu = 1.5\times10^{-6} m^2/sec$ (1.5 cPs), density $\rho = 1000\ kg/m^3$.

Simulation experiments were carried out on fragments of the digital core of cubic shape with linear dimensions of 200 voxels. A cubic cell equal to one voxel was taken as a structural unit of the computational grid. The pressure drop was set to opposite faces of the cube along the x direction in the bedding plane perpendicular to the core axis of the vertical drilling. The pressure P_{in} on the inflow face of the cube is 1.1 kPa and on the outflow $P_{out} = 0.1$ kPa. The component k_x of absolute permeability tensor which is calculated by the equation set below was taken for numerical parameter describing the filtration characteristics of porous media (Barenblatt *et al*., 1984):

$$k_x = \frac{(\sum_{\beta} u_{\beta} dS_{\beta}) \cdot \rho\mu}{(\sum_{\beta} dS_{\beta}) \cdot grad(P)} \quad (3)$$

where, dS is the area of the cell face on the output section and the index "β" number of cells in the outflow section.

RESULTS AND DISCUSSION

Using a mathematical model proposed in this study we have developed a program code which was successfully tested on problems with known analytical solutions: Poiseuille and Couette flow (Loitsianskii, 1973). We also carried out tests on numerical models of porous media Sandstone 1 (S1), Sandstone 3 (S3), Sandstone 5 (S5) and Sand pack (F42B) taken from the open library of core images-Imperial College London (Anonymous, 2015). We further compared the permeability coefficients obtained from the calculations with known values of the filtration characteristics of these samples and showed satisfactory coincidence with a relative error of 10%.

At the first stage, we have investigated the reservoir characteristics of cores with dimensions of 10×4×4 mm. We selected ten samples for the analysis. The spatial tomogram resolution of all cores is 10 μm.

Figures 2a-c show the original image of the tomogram fragment of one of the samples with dimensions of 200×200×200 voxels and its porous structure, revealed as a result of segmentation, respectively. We performed visualization of the processes occurring in the core during the fluid flow with the help of computational experiments conducted by filtering viscous fluid through the test element of the porous medium. The fluid flow features are represented in Fig. 2a-c where the fluid filtration in the

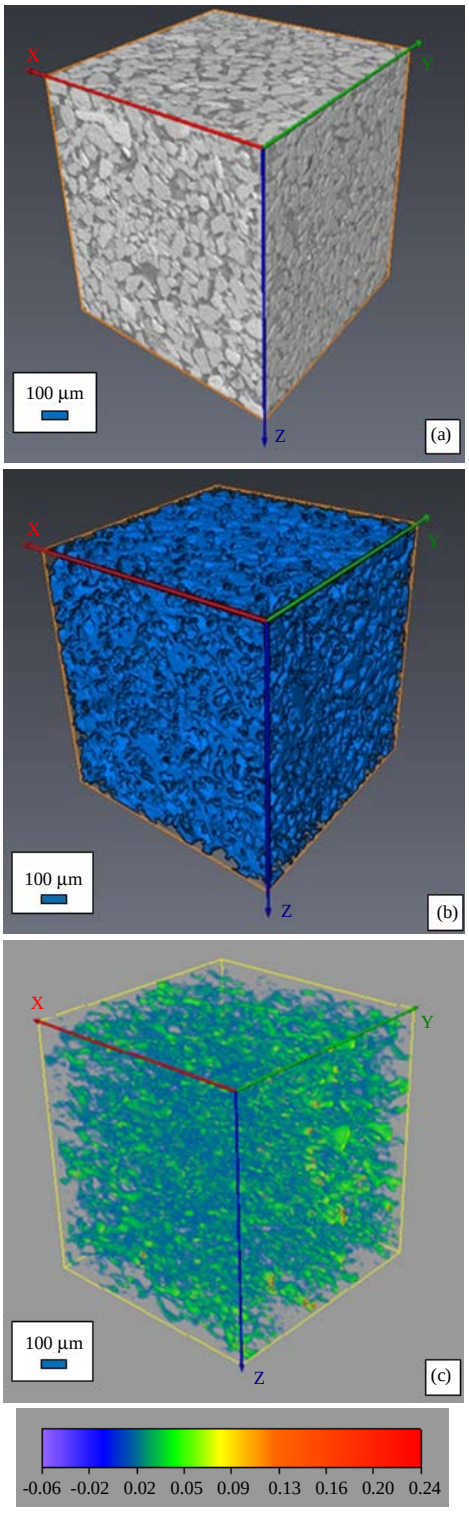

Fig. 2: The results of computational experiments are as follows: a) a digital image of the core; b) the porous structure and c) the field of fluid velocity in the pores (m/sec)

illustrative sample of sandstone is uniformly distributed over the entire core and occurs mainly in the pores with a diameter of 20÷40 μm.

The most common analytical approach for calculation of the absolute permeability coefficient of a porous medium is the use of capillary Kozeny-Carman Model (Romm, 1985). According to Romm (1985), absolute permeability coefficient k_{Carman} depends on the porosity coefficient m and specific pore surface S_V as follows (Mostaghimi *et al*., 2013; Dvorkin *et al*., 2008; Romm, 1985):

$$k_{Carman} = \frac{m^3}{cS_V^2} \quad (4)$$

In Eq. 4, the parameter S_V is calculated as the ratio of pore surface area to sample volume; coefficient c designated as Karman constant, represents the product of two quantities: $c = \gamma \times \varphi^2$ where the coefficient γ characterizes the shape of the channel cross-section and φ-tortuosity of pore channels. Romm (1985) described in his paper the results of experimental works, where the parameter c was calculated from Eq. 4 for the artificial granular porous media with different types of channel cross-sections (circle, ellipse, rectangle, etc.):

$$c = \frac{m^3}{k_{Exp}S_V^2} \quad (5)$$

Experiments have shown that the values of this quantity range 4.7-6.0 (Romm, 1985). The numerical value of the Karman constant c can be also estimated by solving the Navier-Stokes Eq. 1-3:

$$c = \frac{m^3}{k_{NS}S_V^2} \quad (6)$$

Table 1 shows the values of both filtration and capacity parameters, calculated on the basis of digital models of the sandstone segmented tomographic images. Permeability coefficients in column 5 of Table 1 were calculated by the Kozeny-Carman Eq. 4 where c = 5.

As can be seen from column 7, Table 1, Karman constant calculated by the Eq. 6 is in the range (4.0-7.4) which is slightly wider than the interval (4.7-6.0) common to sandstones in papers (Mostaghimi *et al*., 2013; Romm, 1985). We should note that the permeability coefficients calculated by the Kozeny-Carman equation give higher values as compared with the filtration characteristics calculated by Eq. 1-3.

The test cores were previously cut from the traditional 30 mm samples which were also scanned on a tomograph. Coefficients of porosity and permeability were calculated based on the three-dimensional images of 30 mm samples. Despite the fact that the linear resolution of the tomographic images was 32 μ in this case, the measurement results of the properties of 30 mm samples and their corresponding 10 mm samples showed a satisfactory coincidence with the relative difference of not >15%. Based on this result we can conclude that the coefficients of porosity and permeability are determined by the percentage of the largest (>30 μm) pores and channels while the small pores and channels well identified in the 10 μm tomograms have slight effect on these properties. Therefore, the characteristics of cores calculated on the basis of microtomographic data can be extrapolated to the samples of larger porous media.

We have used X-ray computed microtomography to investigate filtration characteristics of a set of cores from sand reservoirs.

We have performed a pore-scaled simulation of the process of viscous fluid flow by using a mathematical model which consists of both the continuity equation and stationary Navier-Stokes equations. We compared the permeability coefficients calculated on the basis of the constructed model with the filtration characteristics calculated by the Kozeny-Carman equation. We have revealed that the permeability coefficients calculated by the Kozeny-Carman equation give higher values as compared with the filtration characteristics calculated by the Navier-Stokes equation.

Table 1: Tomogram-calculated sandstone reservoir properties

Sample name	Porosity (m, rel.un.)	Pore specific surface area S_v (mm^{-1})	Permeability coefficient k_{NS} (μm^2)	Karman permeability coefficient k_{Carman} (μm^2)	Relative deviation $d = 100 \cdot (k_{NS}k_{Carman})/k_{NS}$ (%)	Karman constant, calculated by the Eq. 6
Ss1	0.353	12.56	37.54	55.76	-48.5	7.4
Ss2	0.433	15.66	49.15	66.20	-34.7	6.7
Ss3	0.383	14.73	39.58	51.79	-30.8	6.5
Ss4	0.462	12.42	98.15	127.85	-30.3	6.5
Ss5	0.490	12.76	100.29	144.51	-44.1	7.2
Ss6	0.553	12.44	274.26	218.55	20.3	4.0
Ss7	0.493	13.08	111.83	140.07	-25.3	6.3
Ss8	0.503	12.98	124.63	151.07	-21.2	6.1
Ss9	0.451	11.49	122.71	138.66	-13.0	5.7
Ss10	0.482	18.54	56.93	65.15	-14.4	5.7

It has been shown that the reservoir properties of cores, calculated on the basis of microtomographic data can be extrapolated to the samples of larger porous media.

CONCLUSION

X-ray microtomography is a convenient method not only for visualization of the internal structure of porous media and evaluation of geometric characteristics of the pore space but also for simulation of filtration processes in the scale of pore channels. Spatial resolution of modern microtomographs reaches the size of submicron which allows to calculate the permeability of samples for reservoir fluids (aqueous solutions of salts, oil) within the limited influence of capillary forces occurring in the pore channels with a diameter <5 μm at a reasonable pressure gradient.

ACKNOWLEDGEMENT

The study is performed according to the Russian Government Program of Competitive Growth of Kazan Federal University and RFBR Grant No. «14-01-31096 mol_a».

REFERENCES

Andrew, M., B. Bijeljic and M.J. Blunt, 2014. Pore-scale contact angle measurements at reservoir conditions using X-ray microtomography. Adv. Water Resour., 68: 24-31.

Anonymous, 2015. Micro-CT images and networks. Imperial College London, South Kensington Campus, London, UK.

Barenblatt, G.I., V.M. Entov and V.M. Ryzhik, 1984. Movement of Liquids and Gases in Natural Reservoirs. Nedra, Moscow, Russia, Pages: 207.

Bear, J., 1972. Dynamics of Fluids in Porous Media. 1st Edn., American Elsvier Publishing Company Inc., New York, USA., ISBN-10: 044400114X, pp: 764.

Belotserkovskii, O.M., 1994. Numerical Modeling in Continuum Mechanics. Publishing Company Fiziko-Matematicheskaia Literatura, Moscow, Russia, Pages: 443.

Blunt, M.J., B. Bijeljic, H. Dong, O. Gharbi and S. Iglauer *et al*., 2013. Pore-scale imaging and modelling. Adv. Water Resour., 51: 197-216.

Bulgakov, G.T., A.R. Sharifullin, R.I. Kharisov, A.V. Baizigitova, A.G. Telin and A.V. Pestrikov, 2010. Laboratory and technical studies of carbonate acid treatment. Oil Ind., 4: 2-6.

De Boever, E., C. Varloteaux, F.H. Nader, A. Foubert, S. Bekri, S. Youssef and E. Rosenberg, 2012. Quantification and prediction of the 3D pore network evolution in carbonate reservoir rocks. Oil Gas Sci. Technol., 67: 161-178.

Dvorkin, J., M. Armbruster, C. Baldwin, Q. Fang and N. Derzhi *et al*., 2008. The future of rock physics: Computational methods vs. lab testing. First Break, 26: 63-68.

Farber, L., G. Tardos and J.N. Michaels, 2003. Use of X-ray tomography to study the porosity and morphology of granules. Powder Technol., 132: 57-63.

Gosmen, A.D., V.M. Pan, A.K. Ranchel, D.B. Spalding and M. Wohlstein, 1972. Research Numerical Methods of the Viscous Liquid Flows. Nedra, Moscow, Russia, Pages: 324.

Iassonov, P., T. Gebrenegus and M. Tuller, 2009. Segmentation of X-ray computed tomography images of porous materials: A crucial step for characterization and quantitative analysis of pore structures. Water Resour. Res., Vol. 45, No. 9. 10.1029/2009WR008087.

Kuper, K.E., D.A. Zedgenizov, A.L. Ragozin, V.S. Shatsky and V.V. Porosev *et al*., 2007. Three-dimensional distribution of minerals in diamondiferous eclogites, obtained by the method of high-resolution X-ray computed tomography. Nuclear Instrum. Methods Phys. Res. Sect. A: Acceler. Spectrom. Detectors Assoc. Equip., 575: 255-258.

Loitsianskii, L.G., 1973. Fluid and Gas Mechanics. Nauka, Moscow, Russia, Pages: 848.

Mathews, J.P., J.D.N. Pone, G.D. Mitchell and P. Halleck, 2011. High-resolution X-ray computed tomography observations of the thermal drying of lump-sized subbituminous coal. Fuel Process. Technol., 92: 58-64.

Mostaghimi, P., M.J. Blunt and B. Bijeljic, 2013. Computations of absolute permeability on micro-CT images. Math. Geosci., 45: 103-125.

Nikiforov, A.I., T.R. Zakirov and G.A. Nikiforov, 2015. Model for treatment of oil reservoirs with polymer-dispersed systems. Chem. Technol. Fuels Oils, 51: 105-112.

Nikolaevskii, V.N., 1996. Geomechanics and Fluid Dynamics. Nedra, Moscow, Russia, Pages: 448.

Roach, P., 1980. Computational Hydrodynamics. Publishing House Mir, Moscow, Russia, Pages: 608.

Romm, E.S., 1985. Structural Models of the Pore Space of Rocks. Nedra, Leningrad, Russia, Pages: 240.

Saad, Y., 2003. Iterative Methods for Sparse Linear Systems. 2nd Edn., Society for Industrial and Applied Mathematics, Philadelpha, PA., USA., ISBN-13: 978-0898715347, Pages: 528.

Watanabe, N., T. Ishibashi, Y. Ohsaki, Y. Tsuchiya and T. Tamagawa *et al*., 2011. X-ray CT based numerical analysis of fracture flow for core samples under various confining pressures. Eng. Geol., 123: 338-346.

Wennberg, O.P., L. Rennan and R. Basquet, 2009. Computed tomography scan imaging of natural open fractures in a porous rock; geometry and fluid flow. Geophys. Prospecting, 57: 239-249.

Zakirov, T.R. and A.I. Nikiforov, 2012. Modeling acid impact in water flooding oil reservoir. Oil Ind., 6: 62-65.

Zakirov, T.R. and A.I. Nikiforov, 2013. Simulation of waterflood acid exposure in the near-well zone of the oil reservoir. Math. Simul., 25: 54-63.

Zakirov, T.R. and A.I. Nikiforov, 2014. Simulation of heat treating the oil collector using acid exposure on near-Wellbore zone. Oil Ind., 10: 60-63.

Zakirov, T.R., A.I. Nikiforov and A.I. Latypov, 2015. Modeling thermal treatment in combination with acid treatment of a multilayer oil reservoir. Chem. Technol. Fuels Oils, 50: 547-554.